

Article

Hall-Sensor-Based Position Detection for Quick Reversal of Speed Control in a BLDC Motor Drive System for Industrial Applications

Mohanraj Nandakumar ^{1,*} , Sankaran Ramalingam ¹, Subashini Nallusamy ¹ and Shriram Srinivasarangan Rangarajan ^{1,2,*}

¹ Department of EEE, SASTRA Deemed to be University, Thanjavur, Tamil Nadu 613401, India; rs@eee.sastra.ac.in (S.R.); nmnsi@eee.sastra.ac.in (S.N.)

² Department of Electrical and computer Engineering, Clemson University, Clemson, SC 29634, USA

* Correspondence: snehammohan@eee.sastra.edu (M.N.); shriras@g.clemson.edu (S.S.R.)

Received: 17 June 2020; Accepted: 14 July 2020; Published: 16 July 2020



Abstract: This paper proposes the novel idea of eliminating the front-end converters used indirect current (DC) bus voltage variation, thereby allowing for control of the speed of the brushless direct current (BLDC) motors in the two-quadrant operation of a permanent magnet brushless direct current (PMBLDC) motor, which is required for multiple bi-directional hot roughing steel rolling mills. The first phase of steel rolling, the manufacture of plates, strips etc., using hot slabs from the continuous casting stage, is carried out for thickness reduction, before the same is sent to the finishing mill for further mechanical processing. The hot roughing process involves applying high, compressive pressure, using a hydraulically operated mechanism, through a pair of backup rolls and work rolls for rolling. Overall, the processes consist of multiple passes of forward and reverse rolling at increasing roll speeds. The rolling process was modeled, taking into account parameters like roller dimensions, angle and length of contact, and rolling force, at various temperatures, using actual data obtained from a steel mill. From this data, speed and torque profiles at the motor shaft, covering the entire rolling process, were created. A profile-based feedback controller is proposed for setting the six-pulse inverter frequency and parameters of the pulse width modulated (PWM) waveform for current control, based on Hall sensor position, and the same is implemented for closed loop operation of the brushless direct current motor drive system. The performance enhancement of the two different controllers was also evaluated, during the rolling of 1005 hot rolled (HR) steel, and was taken into consideration in the research analysis. The entire process was simulated in the MATLAB/Simulink platform, and the results verify the suitability of an entire-drive system for industrial steel rolling applications.

Keywords: Hall sensors; brushless direct current motor drive system; power electronics; industrial application

1. Introduction

Steel manufacturing is a highly power-intensive process, wherein about 8% of the total energy consumption is absorbed in hot steel rolling. During the beginning stage of the rough rolling mill, steel slabs from the continuous casting stage are rolled to produce products like plates or strips. Subsequent stages use the above intermediate products for production of thin sheets and similar items. In order to eliminate oxide layers, the hot steel slab specimen has to undergo surface cleaning by means of scrubbing. With the deployment of high-powered electric motors using a gear train arrangement, the set of work and backup rolls are initiated. The physical parameters of the material, like the

dimensions of the roller, the work temperature, and the metallurgical properties, are considered during the rolling process, while the torque and rolling force need to be calculated during the multi-pass operation. Profiles involving forward–reverse rolling based on the above calculations facilitate fixing the speed of the shaft and the torque that constitute the operating points of the motor that is driving.

The choice of electric motors includes induction-based motors, synchronous motors, and direct current (DC) motors. Among the various motors, a specially designed motor called the Brushless direct current motor is preferred, based on inherent features like low maintenance, owing to the absence of brushes, no sparking, and less wear and tear.

The modeling of the closed loop drive system, along with a controller using speed and current feedback, integrated with equations governing the steel rolling process, is presented in this paper. A Simulink [1] schematic of the drive system was created to meet the requirements of the work profile. The performance characteristics of the drive motor were ascertained for ten passes of steel rolling. The characteristics involving the back EMF (electromotive force), such as the current of the stator, the speed of the shaft, and the electromagnetic torque are clearly manifested in this paper by means of simulation.

2. Model of a Rolling Mill

Figure 1 shows a simplified schematic of a typical rough rolling mill for handling hot steel slabs for thickness reduction. The Brushless Direct Current (BLDC) motor [2] drive operates the system of backup rolls, the pair of work rolls, and a gear train [3] mechanism. The above drive system is made up of a four-pole BLDC motor [4] and a six-pulse inverter fed from a DC source. The control configuration senses the speed error signal, which is processed through a Proportional plus Integral controller to generate reference torque. The actual stator current is compared with the generated reference current for producing logic and timing signals required for gate control of the six-pulse IGBT inverter.

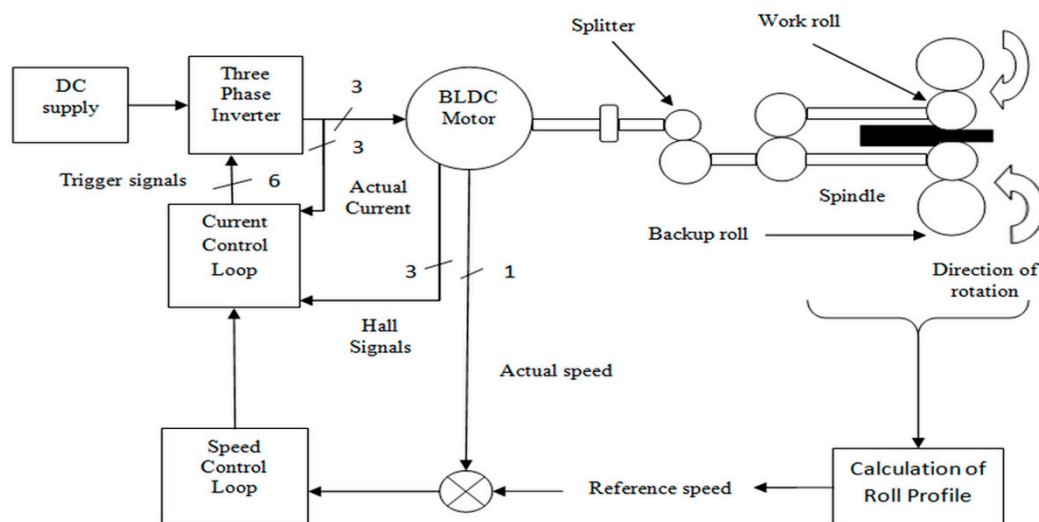


Figure 1. Direct current (DC) motor drive system coupled to a hot rough rolling mill.

2.1. Formulae Governing the Hot Rolling Process

The deformation due to the rolling of a hot slab of steel (which is known by the term draft D) leading to the reduction of thickness of the material [5,6], under specified operating conditions, is governed by the following equation:

$$D = T_I - T_F \quad (1)$$

where D = draft in mm; T_I = starting thickness in mm; and T_F = final thickness in mm.

The work piece under consideration is rolled based on thickness, with ϵ being the true strain whose equation, before and after the rolling of the work material, is given by

$$\epsilon = \ln\left(\frac{T_I}{T_F}\right). \tag{2}$$

The following equation is used to compute the average flow stress (\bar{Y}_f) on the work material during flat rolling, where K is the strength coefficient of the material in MPa, and n is the strain-hardening exponent obtained as in Figures 2 and 3 for 1005 Hot Rolled steel material:

$$\bar{Y}_f = \frac{K\epsilon^n}{1+n} \tag{3}$$

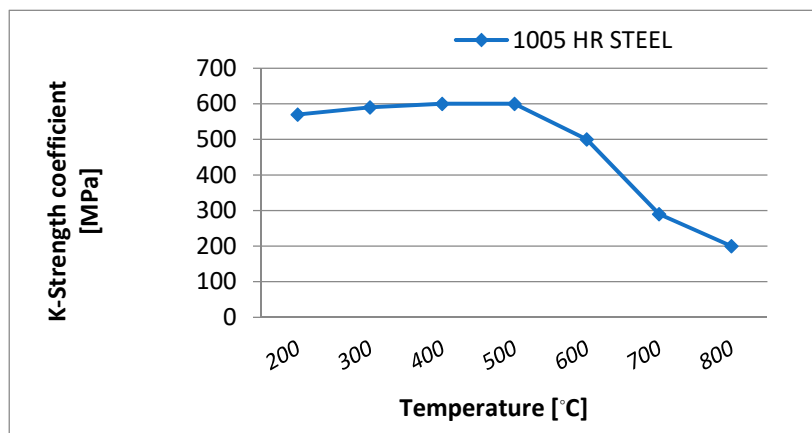


Figure 2. Coefficient versus temperature for a 1005 hot rolled steel specimen.

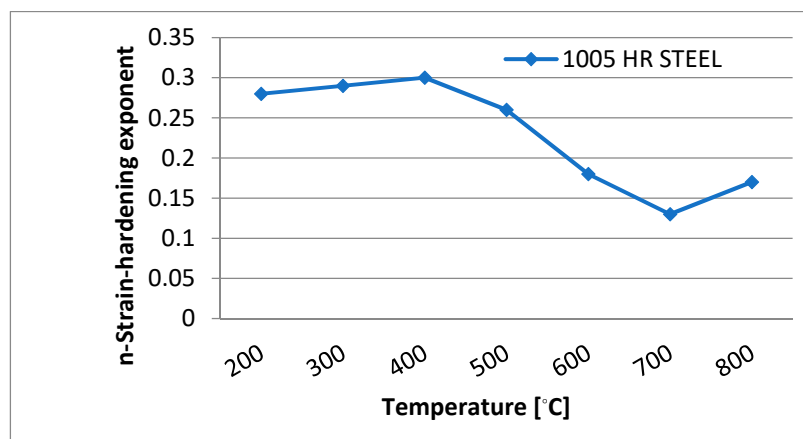


Figure 3. Exponent versus temperature for a 1005 hot rolled steel specimen.

The contact length (C_L) is given by

$$C_L = [R_R (T_I - T_F)]^{0.5} \tag{4}$$

where R_R = Radius of the work roll in mm.

Rolling force (F) is given by

$$F = \bar{Y}_f w C_L \tag{5}$$

where w = steel slab width in mm.

Load torque (T_L) is given by which is related to force as follows:

$$T_L = FC_L \quad (6)$$

2.2. Rolling Process Parameters

For the low carbon specimen of 1005 HR steel [7,8], the metallurgical data and parameters [9] were obtained from the standard ASM Metals Handbook and shown in Table 1. Figure 2 shows the variation of the strength coefficient (K) and Figure 3 the strain hardening coefficient (n) with respect to temperature in °C.

Table 1. Mechanical properties of 1005 HR Steel.

Properties	1005 HR Steel
Density (gr/cm ³)	7.872
Modulus of Elasticity (GPa)	210
Yield strength (MPa)	>280
Poisson's ratio	0.27 to 0.3
Break Elongation (%)	28 (in 80 mm)
Hardness, Vickers	105
Tensile strength (MPa)	325

The actual rolling of the steel slab [10] was carried out in a forward–reverse manner, cyclically, over 10 passes with successive thickness reductions and increases in roll speed, as shown in Table 2.

Table 2. Rolling parameters for ten passes.

Pass	Temperature, °C	K, MPa	n
1	800	200	0.18
2	795	205	0.177
3	790	210	0.174
4	785	215	0.171
5	780	220	0.168
6	775	225	0.165
7	770	230	0.162
8	765	235	0.159
9	760	240	0.156
10	750	245	0.153

3. Creation of Speed and Torque Values

The speed and torque values were deduced from the equations formed from the hot rolling process by employing various values from the graphs of the strength coefficient versus temperature, and the strain hardening exponent versus temperature. It is desirable for the thickness reduction to be performed at a higher speed, provided that the operation is quick and utmost care is taken, as a slight reduction in temperature causes hardening of the hot specimen. Hence, several passes are suggested for rolling operations and the direction of rotation of the work roll reverses at the end of the work specimen, which also makes the steel slab move in the reverse direction. This action is repeated several times to realize multiple-roll operation. Alternate positive and negative values were acquired from both the torque and drive speed, corresponding to the 1st and 3rd quadrant operation of the BLDC motor [11–13]. Table 3 indicates the values of roller speed, motor speed, shaft torque, and thickness reduction for the total time duration of 50 s.

Table 3. Profile values of speed and torque (operation: 10 passes).

Roller Speed (RPM)	Motor Speed (RPM)	Shaft Torque (N-m)	Reduced Thickness (cm)	Time Duration (s)
20	800	423	9.7	5
−20	−800	−432	9.4	5
22.5	900	449	9.1	5
−22.5	−900	−466	8.8	5
25	1000	483	8.5	5
−25	−1000	−500	8.2	5
27.5	1100	518	7.9	5
−27.5	−1100	−536	7.6	5
30	1200	555	7.3	5
−30	−1200	−575	7.0	5

4. Feedback Controller Design

The profile values from Table 3 are the specific values of torque and speed for the steel rolling operation of the mill. The BLDC drive should confine its operation to the required stator current and inverter frequency. This was effected by means of a suitable controller, and a suitable inner and outer control loop. A PI controller was used in the loops. Speed error was processed in the outer loop of the controller, which produced a reference for the torque, in order to generate the three phase currents that were used as a further reference in the control mechanism as follows:

$$\omega_e(t) = \omega^*(t) - \omega_{act}(t) \quad (7)$$

$$T^*(t) = K_p \omega_e(t) + K_i \int_0^t \omega_e(t) \quad (8)$$

$$I^*(t) = \frac{T^*(t)}{K_t} \quad (9)$$

$$I_a^*(t) = I^*(t)0^\circ \quad (10)$$

$$I_b^*(t) = I^*(t) - 120^\circ \quad (11)$$

$$I_c^*(t) = I^*(t) - 240^\circ. \quad (12)$$

The actual values of the phase currents belonging to the motor were compared with the above generated reference currents, involving a bang-bang control for limiting the signal within the hysteresis band, for further generation of six gating pulses for the three-phase inverter [2]. The first and third quadrant operation of the brushless DC motor, for both forward and reverse operation was governed by profile values of speed and torque, with polarity reversal in the rolling operation. Suitable parameters for the controller were chosen for the smooth operation of the entire system.

5. Schematic of the Modeled System

The MATLAB/Simulink simulation platform was employed to carry out the modeling of the hot roughing steel rolling mill, as depicted in Figure 4. Along with the various parameters of the process model, torque–speed profile values at the motor shaft over ten passes, as shown in Table 3, were specified. These profile data [14–16] correspond to the operating conditions during multi-cyclic, forward–reverse runs of rolling being carried out [17,18].

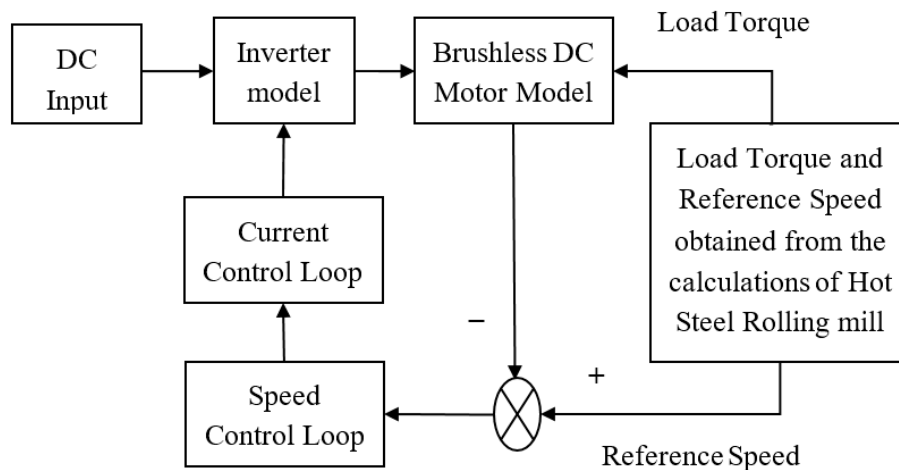


Figure 4. The entire closed loop system in Simulink.

Simulation Results

A simulation run was captured for a period of 50 s, portraying the stator current, back EMF, electromagnetic torque, and speed of the rotor.

Figure 5 shows the simulation results of the rolling operation over an entire period of 50 s for ten passes, depicting the first and third quadrant operation of the BLDC drive system following the speed profile.

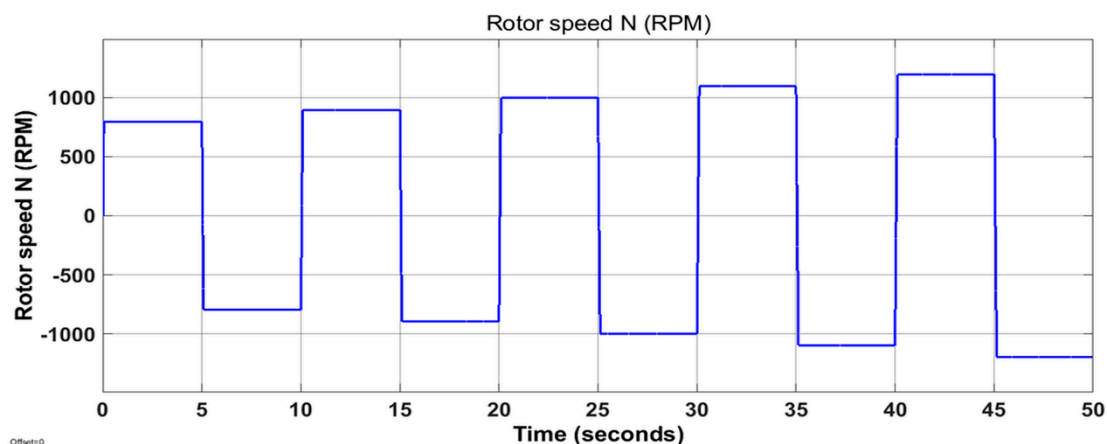


Figure 5. Speed over a period of 50 s.

In Figure 6, the back-EMF waveform is shown for 50 s over ten passes, depicting the first and third quadrant operation of the BLDC drive system. Its expanded view, which is trapezoidal, is shown over a particular period in Figure 7.

The waveform shown in Figure 8 depicts the simulated output of the electromagnetic torque over an entire period of 50 s and for the ten passes required for the first and third quadrant operation of the BLDC drive system [19,20] following the torque profile.

The efficacious nature of the controller is clearly demonstrated in the rapid reversal involved, with respect to the torque and speed characteristics, needed during the rolling process, as shown in Figures 5 and 8. As the rolling process progresses, the quick response of the drive system for bidirectional rolling clearly presents a series of stepped increases of all variables over successive periods.

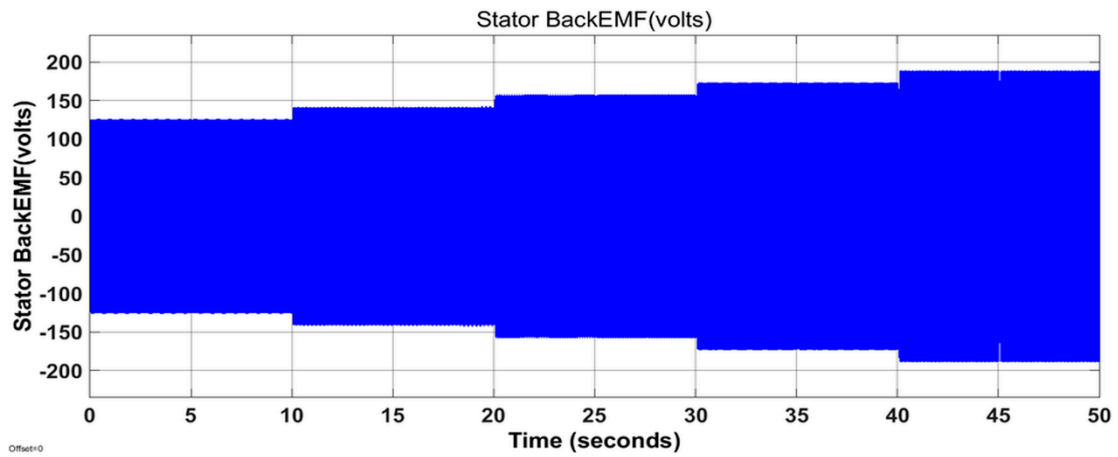


Figure 6. Back-Electro Motive Force waveform in phase A over 50 s.

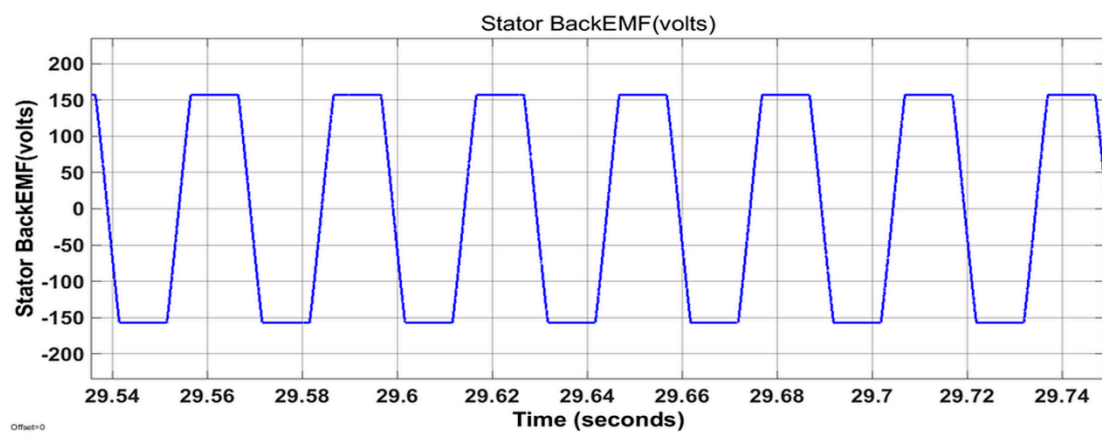


Figure 7. View of the motor's back electromotive force waveform.

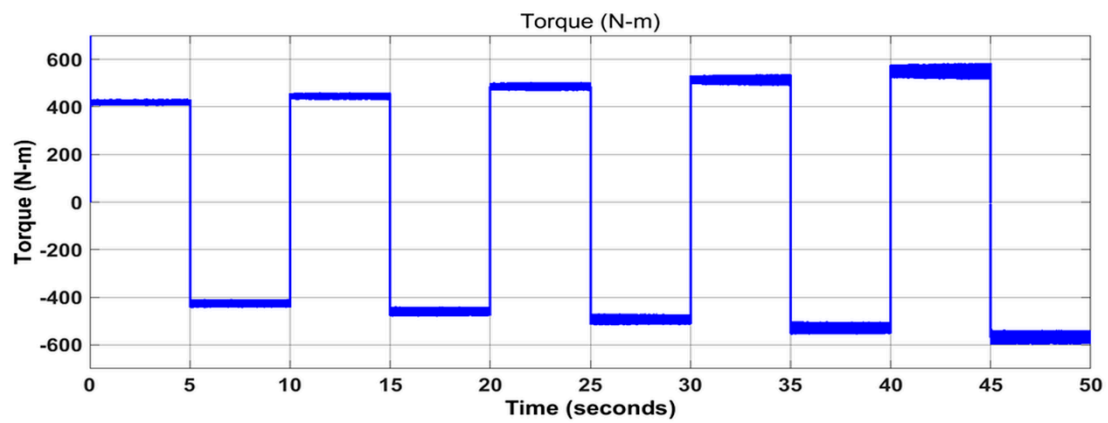


Figure 8. Torque over 50 s.

The stator current waveform, shown in Figure 9, depicts the simulation results for an entire period of 50 s, over ten passes, and its expanded view is also shown in Figure 10, over a particular period, which is rectangular in shape.

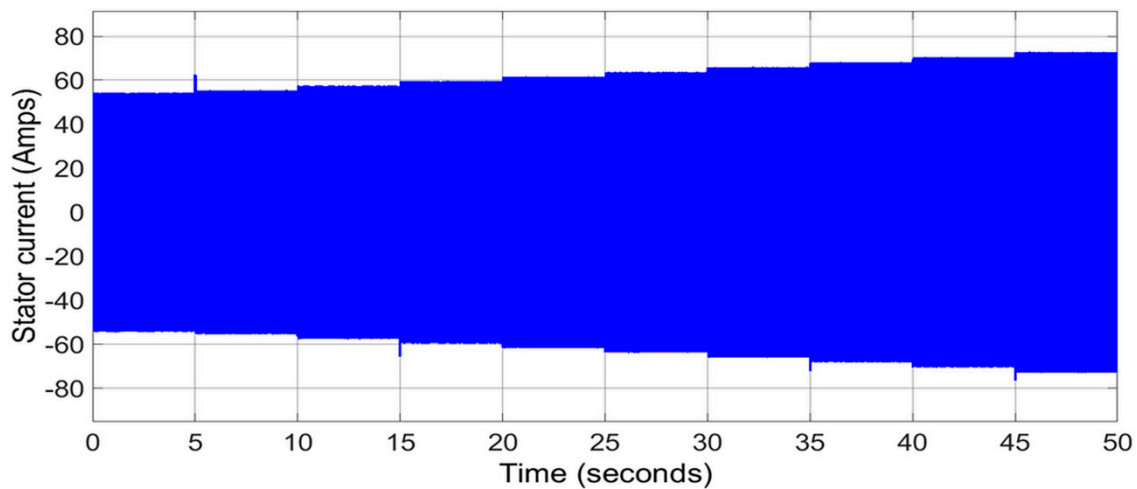


Figure 9. Current waveform over 50 s.

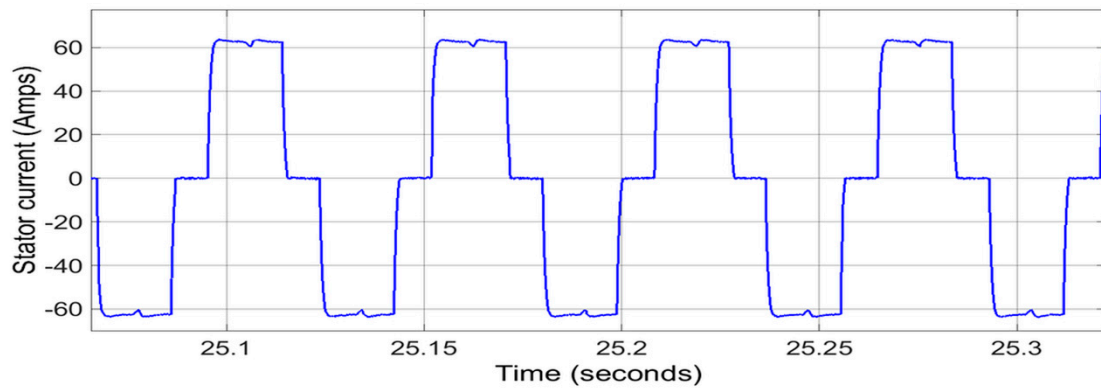


Figure 10. View of the stator’s current waveform.

A profile-based feedback controller is proposed for setting the six-pulse inverter frequency and parameters of the PWM waveform for current control based on Hall sensor position, and the same is implemented for the closed loop operation of the brushless direct current motor drive system. The speed response of the two different controllers, controller 1 and controller 2, are shown in Figure 11, and its expanded view depicts that controller 2 provided a smoother response compared with controller 1. In contrast, controller 1 has a higher amount of overshoot, which is quite evident in the expanded view. Moreover, controller 1 and controller 2 had different gain parameters selected for obtaining better performance.

Table 4 shows the ratings and parameters of the BLDC motor used in this paper.

Table 4. Brushless direct current (BLDC) motor parameters.

Back EMF Motor Rating	Trapezoidal62 HP
Voltage	3-phase, 440 V
Rated Speed	1500 RPM
Resistance (Phase)	0.21 Ω
Inductance (Phase)	8.5 mH
Number of pole pairs	2

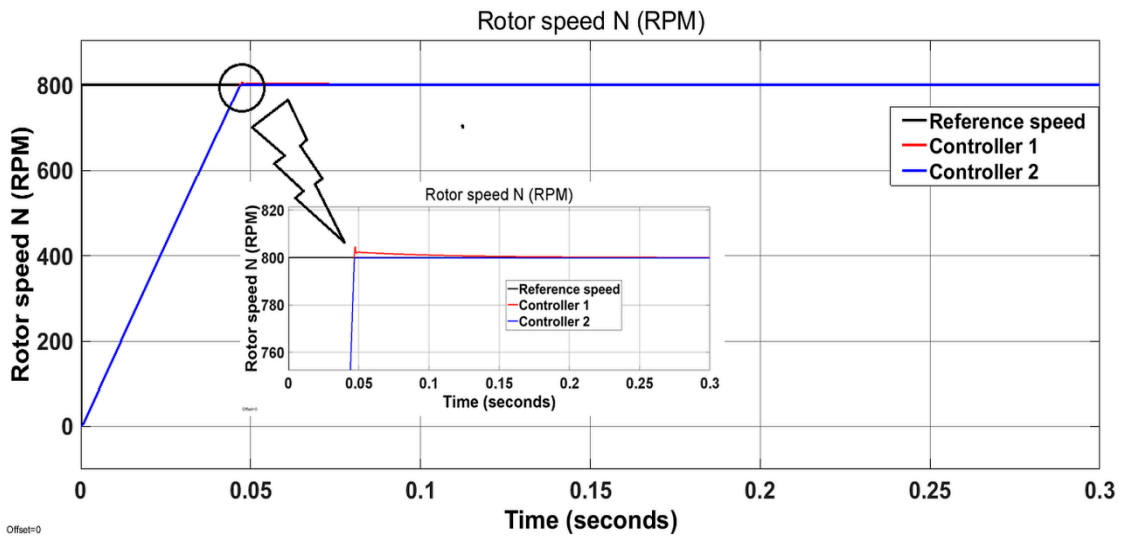


Figure 11. Rotor speed of the two different controllers following the speed profile, and its expanded view.

6. Hardware Setup

Figure 12 illustrates the hardware setup of the drive system employed for the research, in a laboratory-based environment. It consisted of an IGBT-based intelligent power module (IPM), the brushless direct current (BLDC) motor belt coupled to a direct current (DC) generator, and the load arrangements. For the drive system to operate in a closed-loop mechanism, an ARM development board with speed sensors and interfaces was employed. A three-phase alternating current (AC) supply fed the bridge rectifier for obtaining the DC supply to drive the BLDC motor. The generated reference parameters were compared with the actual parameters, as discussed earlier, by means of a suitable controller mechanism. A CPU that was interfaced with the BLDC motor drive system was employed for monitoring the actual and reference speeds. This can be clearly observed from the screen display in Figure 12.



Figure 12. Brushless DC motor drive hardware arrangements.

The actual rotor speed of the BLDC motor, following the set or reference speed is shown in Figure 13. The reference speed ranges from 900 RPM to 1300 RPM, with incremental steps of 100 RPM. A red-colored line indicates the reference or set speed, which was set by the user and accordingly the motor speed tracked the set speed indicated in a blue color.

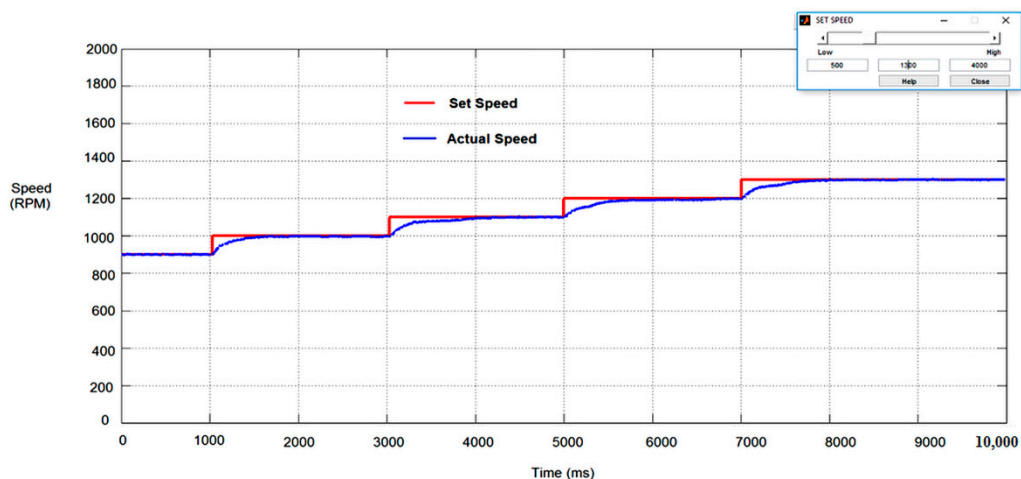


Figure 13. Actual speed of brushless DC motor tracks increased values of set speed viewed in a Graphical User Interface (GUI).

The forward motion of the Brushless DC motor tracked the set or reference speed with decreasing values spanning from 1300 RPM to 900 RPM in steps of 100 RPM, as shown in Figure 14.

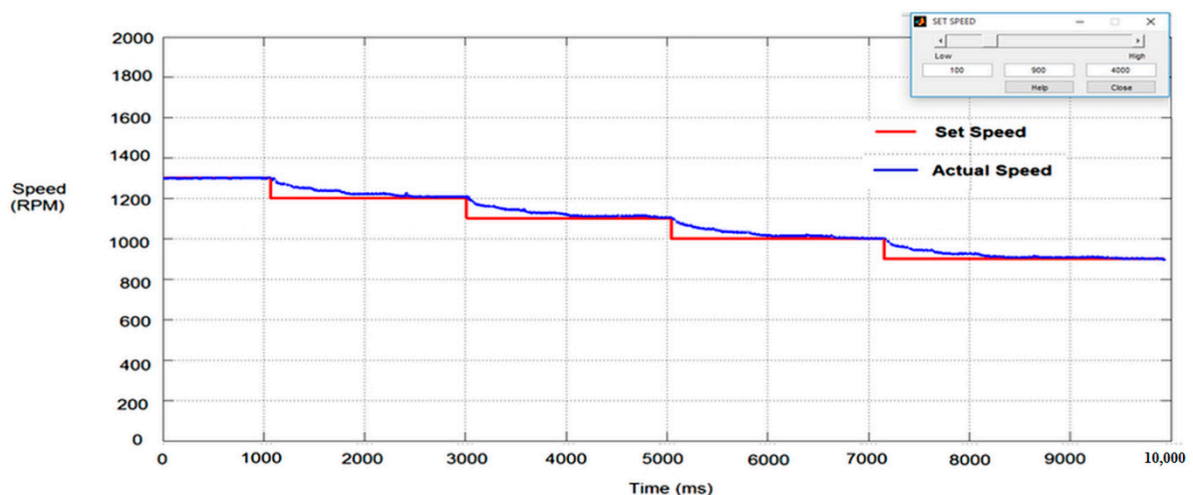


Figure 14. Actual speed of the brushless DC motor tracked decreasing values of set speed, as viewed in the GUI.

7. Conclusions

A total system for hot rough steel rolling, consisting of a BLDC motor drive, coupled to a set of work rolls and backup rolls, along with a closed loop controller, with a multi-loop configuration has been presented in this paper. The set of mathematical equations covering the steel rolling process, the BLDC motor model, and the controller model have been developed for simulation. The simulation results, corresponding to the first and third quadrant operation of the BLDC motor drive system, for a multi-pass steel roughing mill of a 1005 hot rolled steel feed specimen, have been obtained. A profile-based controller has been successfully employed for the smooth operation of the entire system. Furthermore, the performance of the drive system proved it to be an efficient mechanism for fast hot rolling. Hence, it is concluded that a BLDC-motor-based drive system, as presented in this paper, can serve as a powerful replacement for the traditional induction motor drive systems that have been employed for steel rolling, thereby eliminating the need for front-end converters, which in turn eliminates the cost of equipping the components used in them, and, thus, also improving the conversion efficiency.

Author Contributions: M.N. performed the work under the guidance and direction of S.R., S.N. and S.S.R. All authors analyzed the data and contributed towards the paper. M.N. wrote the paper and executed the experiments under the guidance and supervision of, and with suggestions from, S.R., S.N. and S.S.R. All authors also have contributed towards writing and editing the paper. All authors have read and agreed to the published version of the manuscript.

Funding: This research received no external funding.

Acknowledgments: The authors thank the SASTRA Deemed University for providing all of the facilities in the research lab of Power Electronics & Drives that were used to carry out the research.

Conflicts of Interest: The authors declare no conflict of interest.

References

1. Math Works. The Math Works—MATLAB and Simulink for Technical Computing. 2016. Available online: <http://www.mathworks.com> (accessed on 7 September 2016).
2. Gamazo-Real, J.C.; Vázquez-Sánchez, E.; Gómez-Gil, J. Position and Speed Control of Brushless DC Motors Using Sensorless Techniques and Application Trends. *Sensors* **2010**, *10*, 6901–6947. [[CrossRef](#)] [[PubMed](#)]
3. Mahfouf, M.; Yang, Y.Y.; Gama, M.A.; Linkens, D.A. Roll speed and Roll Gap control with Neural Network Compensation. *ISIJ Int.* **2005**, *45*, 841–850. [[CrossRef](#)]
4. Masood, R.J.; Wang, D.B.; Ali, Z.A.; Khan, B. DDC Control Techniques for Three-Phase BLDC Motor Position Control. *Algorithms* **2017**, *10*, 110. [[CrossRef](#)]
5. Chattopadhyay, A.K. Alternating Current Drives in the Steel Industry, Advancements in the last 30 years. *Ind. Electron. Mag.* **2010**, *4*, 30–42. [[CrossRef](#)]
6. Kun, E.; Szemmelveisz, T. Energy efficiency enhancement in the Hot Rolling Mill. *Mater. Sci. Eng.* **2014**, *3*, 4350.
7. Rodríguez, J.R.; Pontt, J.; Newman, P.; Musalem, R.; Miranda, H.; Morán, L.; Alzamora, G. Technical Evaluation and Practical Experience of High-Power Grinding Mill Drives in Mining Applications. *IEEE Trans. Ind. Appl.* **2005**, *41*, 866–873. [[CrossRef](#)]
8. Lotter, U.; Schmitz, H.-P.; Zhang, L. Application of the Metallurgically Oriented Simulation System “TKS-StripCam” to predict the properties of Hot Strip Steels from the Rolling Conditions. *Adv. Eng. Mater.* **2002**, *4*, 207–213. [[CrossRef](#)]
9. Yamada, F.; Sekiguchi, K.; Tsugeno, M.; Anbe, Y.; Andoh, Y.; Forse, C.; Guernier, M.; Coleman, T. Hot Strip Mill Mathematical models and SetUp Calculation. *IEEE Trans. Ind. Appl.* **1991**, *27*, 131–139. [[CrossRef](#)]
10. Orcajo, G.A.; Rodríguez, J.; Ardura, P.; Cano, J.M.; Norniella, J.G.; Llera, R.; Cifrián, D. Dynamic Estimation of Electrical Demand in Hot Rolling Mills. In Proceedings of the IEEE Industry Applications Society Annual Meeting 2015, Dallas, TX, USA, 18–22 October 2015.
11. Gieras, J.F. *Permanent Magnet Motor Technology, Design and Applications*; Second Edition Revised and Expanded; CRC Press: Boca Raton, FL, USA, 2002.
12. Niknejad, P.; Agarwal, T.; Barzegaran, M.R. Utilizing Sequential Action Control Method in GaN-Based High-Speed Drive for BLDC Motor. *Machines* **2017**, *5*, 28. [[CrossRef](#)]
13. Miller, T.J.E. *Brushless Permanent Magnet & Reluctance Motor Drives*; Clarendon Press: Oxford, UK, 1989; Volume 2, pp. 192–199.
14. ASM International. *ASM Metals Handbook, Vol.14, Forming and Forging*; ASM International: Novelty, OH, USA, 1996; pp. 351–355.
15. Groover, M.P. *Fundamentals of Modern Manufacturing. Materials, Processes and Systems*, 4th ed.; John Wiley & Sons: Hoboken, NJ, USA, 2010; pp. 395–403.
16. *AISI/SAE Standard (American Iron and Steel Institute/Society of Automotive Engineers)*; SAE J403 1050; SAE: Warrendale, PA, USA, 2014.
17. Cunkas, M.; Aydoğdu, O. Realization of Fuzzy Logic Controlled Brushless DC Motor Drives Using Matlab/Simulink. *Math. Comput. Appl.* **2010**, *15*, 218–229.
18. Singh, B.; Bist, V. An improved power quality bridgeless Cuk converter fed BLDC motor drive for air conditioning system. *IET Power Electron.* **2013**, *6*, 902–913. [[CrossRef](#)]

19. Pillay, P.; Krishnan, R. Modeling, simulation, and analysis of permanent- magnet motor drives, part II: The brushless dc motor drive. *IEEE Trans. Ind. Appl.* **1989**, *IA-25*, 274–279. [[CrossRef](#)]
20. Nandakumar, M.; Ramalingam, S.; Nallusamy, S.; Rangarajan, S.S. Novel efficacious utilization of Fuzzy Logic Controller based Two-quadrant operation of PMBLDC Motor Drive System for Multi-Pass hot steel rolling Process. *Electronics* **2020**, *9*, 1008. [[CrossRef](#)]



© 2020 by the authors. Licensee MDPI, Basel, Switzerland. This article is an open access article distributed under the terms and conditions of the Creative Commons Attribution (CC BY) license (<http://creativecommons.org/licenses/by/4.0/>).